

# Advances in Biomass-Derived Carbon Materials for Energy Storage and Conversion

Huilin Wang ,<sup>a</sup> and Jie Wen <sup>b,\*</sup>

Amid the global energy crisis and the pursuit of carbon neutrality, biomass-derived carbon materials (BDCs) have emerged as promising sustainable candidates for energy applications due to their abundant sources, tailororable hierarchical porosity/heteroatom doping, and remarkable properties. This review systematically summarizes recent advances (2020 to 2025) in BDCs for supercapacitors, secondary batteries (lithium/sodium/potassium-ion), and electrocatalysis (ORR/OER/HER/CO<sub>2</sub> RR). The review focuses on the synthesis-structure-performance correlation, highlighting how pore architecture, heteroatom incorporation, and morphology govern electrochemical performance. Key challenges including precursor inconsistency, imperfect structure control, and scalability in sustainable production are critically assessed. Future prospects are proposed, including machine-learning-guided material design, *in situ/operando* mechanistic studies, and practical device integration. This work offers insightful guidance for the rational design of BDCs toward practical energy storage and conversion systems.

DOI: 10.15376/biores.21.2.Wang

Keywords: Biomass-derived carbon materials; Fabrication techniques; Structure tuning strategies; Energy storage; Energy conversion

Contact information: a: College of Landscape Engineering, Suzhou Polytechnic Institute of Agriculture, Suzhou, China; b: Suzhou University of Technology, Suzhou, China;

\* Corresponding author: wenjie@szut.edu.cn

## INTRODUCTION

The depletion of fossil fuels and associated environmental degradation (e.g., greenhouse gas emissions, air pollution) necessitate a global transition toward clean and renewable energy sources (Ma *et al.* 2025; Zhang *et al.* 2025; Zhong *et al.* 2025). Efficient energy storage (e.g., batteries, supercapacitors) and conversion (e.g., fuel cells, water electrolysis) technologies are fundamental pillars enabling this shift, with electrode materials playing a critical role in determining device performance (He *et al.* 2025, 2023). To meet the demands of next-generation energy devices, electrode materials must possess a combination of key attributes: high electrical conductivity for efficient charge transport, tailored porosity for rapid ion diffusion and large surface area, structural stability for long-term cycling, and surface functionalities that facilitate electrochemical reactions. Biomass-derived carbon materials (BDCs) have emerged as promising candidates that can be engineered to meet these criteria, offering a sustainable alternative to conventional carbon materials derived from fossil resources. BDCs are synthesized from abundant, renewable, and often waste resources—including agricultural residues (rice husks, straw), forestry by-products (sawdust, wood), food processing waste (nut shells, fruit pits), and animal/microbial biomass (bones, dung, fungi)—through processes such as pyrolysis,

activation, and hydrothermal carbonization (Hu *et al.* 2024; Liu *et al.* 2025; Roy *et al.* 2025; Wu *et al.* 2024).

BDCs offer several compelling advantages. Their resource abundance and inherent sustainability allow for the valorization of waste streams, aligning with circular economy principles. Their preparation involves core procedures including precursor selection, pretreatment, carbonization, and structural optimization (*e.g.*, activation, templating, pore regulation, and heteroatom doping). By carefully selecting precursor types and controlling synthesis parameters (*e.g.*, activators, temperature, templates), the specific surface area (SSA), pore structure (micropores/mesopores/macropores), and surface chemistry of the resulting materials can be precisely tuned to meet the requirements of specific energy storage and conversion devices (Feng *et al.* 2023; Guo *et al.* 2021; Lu *et al.* 2024; Lv *et al.* 2024; Wu *et al.* 2024). This structural tailorability underpins their excellent physico-chemical properties, encompassing good electrical conductivity, robust chemical/thermal stability, and adequate mechanical strength (Farma *et al.* 2023; Mukherjee *et al.* 2022; Wang *et al.* 2022a). Figure 1 schematically illustrates the structure--property relationships and energy storage applications of biomass-derived carbon (BDC) materials. These versatile carbons are synthesized from diverse biomass precursors such as coconut shells, wood, tea leaves, and pomelo peels. The resulting BDCs exhibit tunable structural characteristics, including heteroatom doping (*e.g.*, N, O, P, S), and hierarchical porous architectures. These features endow the materials with enhanced electrochemical properties, such as high specific capacity/capacitance, excellent cycling stability, and superior rate capability. Consequently, BDCs are promising electrode materials for a wide range of energy storage devices, including lithium-ion batteries, sodium-ion batteries, potassium-ion batteries, and supercapacitors. Furthermore, BDCs present significant environmental and economic benefits due to their low-cost precursors and relatively green preparation routes compared to synthetic carbon materials (*e.g.*, graphene, carbon nanotubes) (Yang *et al.* 2024).

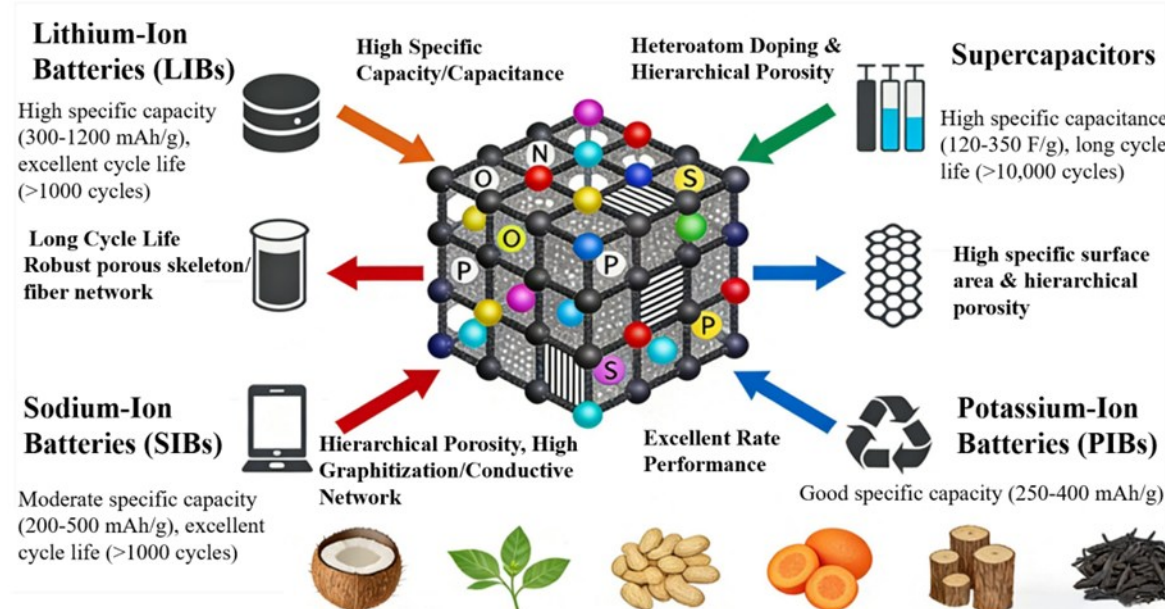


**Fig. 1.** Schematic illustration of structure--performance relationships and energy storage applications of BDCs

Significant advances in the structural design, performance optimization, and mechanistic understanding of BDCs have been made in the past five years, establishing them at the forefront of energy materials research. It is important to note that this review focuses specifically on engineered BDCs designed for electrochemical energy storage and conversion applications, excluding biochar used solely as a solid fuel or agricultural amendment. This review systematically examines recent progress in applying BDCs within three primary domains: supercapacitors, secondary batteries, and electrocatalysis. It critically assesses their performance, structure-property relationships, challenges, and future prospects in each area, with an emphasis on data-driven analysis of key metrics and integration of cutting-edge characterization techniques. This comprehensive resource aims to guide researchers in overcoming current bottlenecks and advancing BDCs toward sustainable energy applications.

## **PREPARATION AND STRUCTURE TUNING STRATEGIES OF BIOMASS-DERIVED CARBON MATERIALS**

### **Fabrication Techniques**

#### *Direct pyrolysis*

This fundamental method involves carbonizing biomass precursors at high temperatures under an inert atmosphere (N<sub>2</sub> or Ar). While straightforward and low-cost, the resulting carbon materials typically exhibit modest specific surface area (SSA < 500 m<sup>2</sup>/g) and underdeveloped porosity. The pyrolysis process can be categorized based on heating rate and temperature, significantly influencing product distribution. Depending on these parameters, the process can be directed toward different outputs: slow pyrolysis prioritizes biochar yield, while fast pyrolysis favors bio-oil production, as shown in Table 1. Mukherjee *et al.* (2022) provide a systematic review of the pyrolysis-mediated conversion of lignocellulosic biomass into biochar, focusing on slow pyrolysis. The work details the correlation between process parameters and biochar properties and evaluates its broad application potential across multiple fields.

#### *Physical activation*

Following initial pyrolysis, the carbon material undergoes secondary activation in an oxidizing atmosphere (CO<sub>2</sub> or steam) at 800 to 950 °C. This process etches the carbon framework to enlarge pores and increase SSA, with steam activation typically producing more mesopores (2 to 50 nm) and CO<sub>2</sub> activation favoring micropores (<2 nm) (Hu *et al.* 2024; Jerez *et al.* 2023). Ding *et al.* (2022) prepared apricot shell-derived activated carbon (AC\_VC-4) via a multi-step physical activation method using steam followed by CO<sub>2</sub>. The obtained material exhibited a well-developed hierarchical porous structure with a total pore volume (V<sub>T</sub>) of 1.40 cm<sup>3</sup>/g, of which 55.9% was contributed by mesopores. Its effective pore volume in the range of 0.8 to 4.0 nm reached 0.720 cm<sup>3</sup>/g. When tested in an EMIMBF<sub>4</sub> ionic-liquid electrolyte, AC\_VC-4 delivered a specific capacitance of 39.2 F/g at 0.5 A/g. These results highlight the feasibility of tailoring pore architecture through designed physical activation processes for improved supercapacitor performance, though the tunability of pore structure *via* physical activation alone remains relatively limited compared to chemical activation. Therefore, physical activation is often combined with chemical methods to achieve more precise and synergistic pore engineering (Hu *et al.* 2024).

**Table 1.** Comparison of Pyrolysis Techniques for Biomass Conversion: Conditions, Target Products, and Resulting Biochar Properties

Technique	Temp. Range (°C)	Heating Rate	Desired Product	Biochar Yield (wt%)	Key Properties of Biochar
<b>Slow Pyrolysis</b>	<b>300 – 700</b> (Common: 400-600)	<b>Slow</b> (0.1 to 10 °C min <sup>-1</sup> )	<b>Biochar</b>	<b>High</b> (25 to 35%)	<b>Dense structure.</b> Low specific surface area (SSA), typically tens to hundreds m <sup>2</sup> /g. <b>Micropore-dominant.</b> Classic method for stable solid carbon.
<b>Fast Pyrolysis</b>	<b>~500</b> (Optimal)	<b>Very Fast</b> (100 to 1000 °C s <sup>-1</sup> )	<b>Bio-oil</b>	<b>Medium-Low</b> (12 to 20%)	<b>More initial pores</b> from violent devolatilization. SSA may be higher than slow pyrolysis char, but <b>lower carbonization degree</b> .
<b>Flash Pyrolysis</b>	<b>&gt; 700</b> (Up to 1200+)	<b>Ultra-Fast</b> (> 1000 °C s <sup>-1</sup> )	<b>Syngas</b>	<b>Very Low</b> (5 to 10%)	Potential <b>graphitization or melting</b> at extreme temperatures. Low SSA. Char is usually a by-product.

Note: The parameters listed represent typical ranges for lignocellulosic biomass and may vary with feedstock composition, reactor type, and process conditions.

### Chemical activation

Chemical activation involves mixing the biomass precursor with activating agents (e.g., KOH, NaOH, ZnCl<sub>2</sub>, H<sub>3</sub>PO<sub>4</sub>) prior to pyrolysis (400 to 900 °C). KOH activation is a widely used method, efficiently etching the carbon framework *via* reactions such as 6KOH + 2C → 2K + 2K<sub>2</sub>CO<sub>3</sub> + 3H<sub>2</sub>↑, yielding high SSA and abundant micro-mesoporosity (Farma *et al.* 2023; Hu *et al.* 2024). For instance, Ding *et al.* (2025) prepared lignin-derived activated carbon *via* KOH activation, achieving a high SSA of 2616 m<sup>2</sup>/g and a specific capacitance of 350 F/g at 1 A/g in 6 M KOH electrolyte. Similarly, Jerez *et al.* (2023) employed a two-step KOH activation method on yerba mate residues to produce activated carbons, achieving a high specific surface area of 1820 m<sup>2</sup>/g and a maximum specific capacitance of 644 F/g at 0.1 A/g---one of the highest values reported for biomass-derived supercapacitor electrodes. The activation mechanism involves complex reactions, including the reduction of KOH to metallic K and the formation of K<sub>2</sub>CO<sub>3</sub>, with the release of gases (e.g., H<sub>2</sub>, CO) creating and expanding pores, as detailed in relevant reviews (Hu *et al.* 2024).

### Hydrothermal carbonization (HTC)

HTC is a mild and energy-efficient pretreatment method that converts wet biomass into a carbon-rich solid (hydrochar) under moderate temperatures (180 to 250 °C) and autogenous pressure. The resulting hydrochar is enriched with oxygenated functional

groups and serves as an excellent precursor for subsequent pyrolysis or activation to fabricate high-performance biomass-derived carbons (BDCs) with tailored porous structures (Hu *et al.* 2024). A key advantage of HTC lies in its ability to engineer the morphology of the carbon precursor. By adjusting core process parameters such as reaction temperature, residence time, biomass concentration, and potential additives, HTC can direct the formation of well-defined morphologies most notably uniform carbon microspheres through mechanisms of polymerization and self-assembly during the hydrothermal process (Hu *et al.* 2010).

Moreover, HTC offers notable potential for resource circularity. Studies have shown that the aqueous process stream (filtrate), which contains abundant soluble organic compounds, can spontaneously yield carbon microspheres under resting conditions. The yield and monodispersity of these self-generated carbon (SGC) particles are significantly enhanced by moderate heating (*e.g.*, up to 50 °C) and gentle agitation (*e.g.*, 30 rpm) (Aveling *et al.* 2025). This presents a promising circular strategy for valorizing a process effluent into low-ash carbon materials.

Collectively, HTC stands as a versatile and sustainable preprocessing step for constructing high-value carbon materials from biomass, while simultaneously advancing the circularity of the conversion process.

### *Templating methods*

Template carbonization is a pivotal strategy for engineering the porosity of biomass-derived carbons (BDCs) with high precision. This technique involves incorporating sacrificial templates (hard or soft) into the biomass precursor. Subsequent carbonization and template removal yield a porous carbon matrix whose architecture is a direct replica of the template, enabling unparalleled control over pore size, volume, and connectivity.

Hard-templating employs solid, removable particles (*e.g.*, NaCl, MgO). A representative study by Wang *et al.* (2022) used NaCl crystals as a low-cost, green activating and templating agent mixed with *Artemisia argyi* biomass-derived char. After high-temperature treatment and washing, the NaCl was removed, leaving behind a hierarchically porous carbon. The use of NaCl activation created a high specific surface area (1140 m<sup>2</sup>/g) and an optimal pore structure, which delivered a superb specific capacitance of 348.4 F/g at 1 A/g and exceptional cycling stability (99.7% retention after 20,000 cycles) in a supercapacitor (Wang *et al.* 2022b).

In contrast to hard-templating, the formation of porous structures can also be guided by soft-templating or the intrinsic self-assembly properties of the precursors. A related strategy was demonstrated by Gopalakrishnan and Badhulika (2021), who utilized onion skin waste as a biomass precursor. Through a carbonization process, the natural components within the waste directed the formation of multi-heteroatom self-doped, highly wrinkled porous carbon nanosheets. The resulting carbon material exhibited a well-developed porous structure, delivering a specific capacitance of 245 F/g at 0.5 A/g and excellent cycling stability (94.8% retention after 10,000 cycles) in a supercapacitor (Gopalakrishnan and Badhulika 2021).

The templating concept has been innovatively extended to salt-templating/melt-mediated processes, where inorganic salts act as both the reaction medium and a dynamic “space-filling” template at high temperatures. Zhu *et al.* (2023) systematically summarized the salt-assisted synthesis strategy for advanced carbon-based materials (including those derived from biomass), with typical molten salt systems such as ZnCl<sub>2</sub>-KCl being widely

utilized. In this sustainable one-pot process, the molten salt not only confines the carbonization and etches the matrix to regulate microstructure, but it also serves as an efficient porogen to construct porous structures and even a potential heteroatom dopant source. This versatile method enables the fabrication of carbon materials with tailored morphologies and optimized porous structures. These materials have demonstrated excellent electrochemical performance in energy storage and conversion applications, including supercapacitors, lithium-ion batteries, and also as electrocatalysts, featuring high specific capacity, superior stability, and efficient transport (Zhu *et al.* 2023).

Collectively, templating methods offer a versatile route to precision pore engineering, though they often entail increased synthesis complexity.

Table 2 compares the key characteristics, relative advantages, and limitations of the primary BDC synthesis routes.

**Table 2.** Comparison of Mainstream BDC Preparation Methods

Method	Process Conditions	Product Characteristics	Limitations
<b>Direct Pyrolysis</b>	Inert atmosphere, 500 to 1000 °C	Low SSA (typically < 500 m <sup>2</sup> /g), underdeveloped porosity, but retains initial biomass morphology.	Limited pore development, insufficient for high-performance applications.
<b>Physical Activation</b>	Pyrolysis followed by activation in CO <sub>2</sub> or steam, 800 to 950 °C	Predominantly microporous (CO <sub>2</sub> ) or mesoporous (steam), moderate to high SSA (~1000-1500 m <sup>2</sup> /g), environmentally friendly.	Less tunable porosity and generally lower SSA compared to chemical activation.
<b>Chemical Activation (KOH)</b>	Impregnation with KOH (ratio ≥2:1), 600 to 800 °C	Ultra-high SSA (>2000 m <sup>2</sup> /g), abundant micropores, excellent capacitive performance.	Highly corrosive, requires extensive washing and wastewater treatment.
<b>HTC + Activation</b>	Hydrothermal treatment (180 to 250 °C) + subsequent pyrolysis/activation	Preserved heteroatoms (O, N), tunable morphology (e.g., spheres, sheets), rich in functional groups.	Two-step process, moderate SSA without strong activation.
<b>Template Method</b>	Mixing with hard/soft templates, carbonization at 600 to 900 °C, followed by etching	Ordered pores, tunable architecture (e.g., uniform mesopores), designed structures.	Increased cost and complexity due to template synthesis and removal.

## Structure Tuning Strategies

### Pore structural regulation

Precise pore structure engineering is paramount for unlocking the high-performance potential of biomass-derived carbons in applications like supercapacitors. The overarching goal is to construct a hierarchical pore architecture integrating micropores (<2 nm) for high surface area and charge storage, mesopores (2 to 50 nm) for efficient ion

transport, and macropores ( $>50$  nm) serving as ion reservoirs. This is primarily achieved through chemistry-driven strategies such as chemical activation (e.g., with KOH or  $ZnCl_2$ ) and morphology-directed strategies such as hard/soft templating. Additionally, methods such as hydrothermal carbonization and molten salt carbonization offer complementary routes to tailor the carbon morphology and porosity. The effectiveness of these strategies is evidenced by the dramatic increase in specific surface area (e.g., from 16 to over 1300  $m^2/g$  via KOH activation) and the creation of ordered mesostructures through templating, which collectively enhance electrochemical performance (Wang *et al.* 2017).

The most straightforward method involves selecting specific chemical activating agents. For instance, strong alkalis such as KOH are highly effective in creating extensive microporous networks through vigorous etching, which can lead to materials with very high specific surface areas (often exceeding 2000  $m^2/g$  under optimized conditions, providing the foundation for high capacitance). In contrast, milder agents such as  $KHCO_3$  (or similarly,  $K_2CO_3$ ) favor a more moderate activation process, which tends to generate a higher proportion of ion-accessible mesopores. This pore structure directly enhances the rate of uptake by the material (Hu *et al.* 2024; Wang *et al.* 2017).

Moving beyond the use of a single activating agent, sequential activation with different chemicals has emerged as a powerful strategy to synergistically tailor the pore hierarchy. For example, the order of applying  $ZnCl_2$  and  $H_3PO_4$  in the chemical activation of willow wood can drastically alter the resultant pore structure of the activated carbon, demonstrating that the sequence of chemical treatments is a critical, yet often overlooked, variable in pore engineering (Liang *et al.* 2024). This approach allows for more precise control over the development of micro- and mesopores than single-step activation.

For more precise and tailored porosity, templating approaches and precursor selection are crucial. Utilizing removable hard templates (e.g.,  $MgO$  nanoparticles) allows for direct programming of the pore size distribution. This method can selectively increase the average pore diameter and the proportion of mesopores, leading to a significant improvement in capacitance retention at high current densities (Jiao *et al.* 2025). Furthermore, leveraging the innate anatomical structure of the biomass precursor itself provides a sustainable route to predefined macro- and mesoporous frameworks.

### *Heteroatom doping*

Introducing heteroatoms (N, P, S, B) into the carbon matrix tailors the electronic structure and surface chemistry of biomass-derived carbons (BDCs). This can effectively improve electrical conductivity, electrolyte wettability, and create additional electrochemically active sites (Hu *et al.* 2024). Doping strategies can be intrinsic, by utilizing biomass naturally rich in heteroatoms (e.g., nitrogen-rich animal bones, phosphorus-rich shrimp shells), or extrinsic, via co-pyrolysis with dopant precursors such as urea, thiourea, or boric acid.

Among various heteroatoms, nitrogen (N) doping is the most extensively studied. Different N configurations contribute distinctively to performance: pyridinic N and graphitic N are known to enhance  $\pi$ -electron delocalization (beneficial for conductivity) and create structural defects, while pyrrolic N primarily improves surface wettability. A successful application of N-doping is exemplified by the work of Shang *et al.* (2020), who prepared a nitrogen-doped hierarchically porous carbon from *houttuynia*. The material exhibited a flower-like architecture, a high specific surface area of 2090  $m^2/g$ , and delivered an impressive specific capacitance of 473.5 F/g at 1 A/g. In their study, the doped nitrogen

species were found to collectively improve wettability, provide additional faradic capacity, and enhance conductivity, leading to the outstanding electrochemical performance.

Co-doping with multiple heteroatoms often leads to synergistic effects that further boost performance. For instance, Liu *et al.* (2023a) developed an eco-friendly strategy to prepare oxygen/nitrogen/sulfur (O/N/S) tri-doped, mesopore-dominant porous carbon from *Amygdalus davidiana* shells. The co-doping, along with the high specific surface area (1730 m<sup>2</sup>/g) and mesoporous structure, contributed to favorable surface chemistry and ion transport. The optimal material exhibited a specific capacitance of 208 F/g at 1 A/g in a three-electrode system, demonstrating the effectiveness of multi-heteroatom doping for supercapacitors.

More importantly, nitrogen/phosphorus (N/P) co-doping has proven highly effective for enhancing the oxygen reduction reaction (ORR) activity of carbon materials through synergistic effects. This synergy is ascribed to the modulated electron density distribution and increased defect sites within the carbon matrix, which collectively optimize oxygen adsorption energy and accelerate reaction kinetics. For instance, a study on biomass-derived carbon demonstrated that molasses-derived P, N co-doped carbon exhibited superior ORR performance compared to undoped or singly-doped counterparts. Further introduction of silicon (Si) to create Si, P, N tri-doped carbon provided additional tuning of the pore structure and electronegativity, offering an extended strategy for performance enhancement (Macchi *et al.* 2021). This multi-heteroatom doping approach presents a clear pathway for designing efficient and low-cost metal-free electrocatalysts for ORR.

Heteroatom doping (*e.g.*, N, P, S, or their combinations) significantly enhances the performance of biomass-derived carbons (BDCs) by introducing active sites and modifying electronic structures, as summarized in Table 3.

**Table 3.** Heteroatom Doping Strategies and Performance of BDCs

Doping Element	Doping Source	Key Mechanisms	Representative Performance	Ref.
N	Houttuynia cordata	Provides pseudocapacitive active sites; enhances wettability and conductivity.	SC: 473.5 F g <sup>-1</sup> @ 1 A g <sup>-1</sup> ; CR: 95.7% (10k cycles)	(Shang <i>et al.</i> 2020)
P	Sawdust / H <sub>3</sub> PO <sub>4</sub>	Expands interlayer spacing; P=O functional groups contribute pseudocapacitance.	SC: 292 F g <sup>-1</sup> @ 0.1 A g <sup>-1</sup> ; ED: 10.6 Wh kg <sup>-1</sup>	(Lin <i>et al.</i> 2020)
N, S	Mantis Shrimp Shell	Synergistic N/S effect optimizes electronic structure and pore architecture for enhanced ion transport.	SSA: 3405 m <sup>2</sup> g <sup>-1</sup> ; SC: 456 F g <sup>-1</sup> @ 1 A g <sup>-1</sup>	(Huang <i>et al.</i> 2021)
S	Biomass / Ni <sub>3</sub> S <sub>2</sub> Encapsulation	S-doping modulates electronic structure; encapsulated Ni <sub>3</sub> S <sub>2</sub>	SC: 412 F g <sup>-1</sup> @ 1 A g <sup>-1</sup> ; ED: 56.9 Wh kg <sup>-1</sup>	(Lv <i>et al.</i> 2023)

Doping Element	Doping Source	Key Mechanisms	Representative Performance	Ref.
		provides high Faradaic capacity.		
N, P	Molasses	Creates charge-asymmetric sites (C-P <sup>+</sup> -N), synergistically boosting ORR activity.	ORR HWP: 0.85 V vs. RHE	(Macchi <i>et al.</i> 2021)
O, N, S	Self-doped Precursor	Multi-heteroatom synergy introduces abundant active sites and optimizes hierarchical pore structure.	SC: 386 F g <sup>-1</sup> @ 1 A g <sup>-1</sup> ; CR: 94.2% (10k cycles)	(Liu <i>et al.</i> 2023a)

### *Morphology and dimensional control*

Tailoring the morphology and dimensionality of biomass-derived carbons (BDCs) across zero to three dimensions (0D to 3D) represents a pivotal strategy for optimizing electron/ion transport kinetics and enhancing structural stability in energy storage devices.

Zero-dimensional (0D) structures, such as carbon dots and nanospheres, offer high dispersibility and rich surface functionalization, rendering them ideal for flexible electronics. For instance, Tariq *et al.* (2025) systematically reviewed biomass-derived carbon dots (B-Cdots) synthesized *via* green routes (e.g., microwave-assisted, hydrothermal, and pyrolysis-based carbonization). These B-Cdots possess tunable physicochemical properties, porous structures, and efficient heteroatom doping. They exhibit excellent electrical conductivity and dispersibility, enabling broad applications in supercapacitors, lithium-ion batteries, and sodium-ion batteries, thereby fully exemplifying the structural advantages of 0D materials in sustainable energy storage.

One-dimensional (1D) architectures, including nanotubes and nanofibers, provide continuous pathways that significantly shorten electron transport distances. Liang *et al.* (2021a) fabricated microporous-rich porous carbon frameworks from traditional Chinese medicine residues, which served as efficient sulfur hosts for lithium-sulfur batteries. The continuous 1D structure not only accelerates electron transfer but also suppresses polysulfide shuttling, thereby ensuring long-term cycling stability.

Two-dimensional (2D) materials, such as nanosheets, are highly valued for their large exposed surface area, which facilitates rapid ion diffusion. Xu *et al.* (2020b) proposed a one-step low-cost strategy to synthesize nitrogen/phosphorus (N/P) co-doped large-sized and ultrathin carbon nanosheets from chitosan. Using benign sodium hypophosphite as the phosphorus source and manganese nitrate as both activator and mesoporous template (without additional hard templates), the resulting 2D nanosheets feature a hierarchical porous structure and a high heteroatom doping concentration, providing abundant active sites and unobstructed ion transport channels for supercapacitor applications.

Three-dimensional (3D) monolithic or aerogel networks create interconnected conductive frameworks that ensure mechanical robustness and efficient charge distribution. Ou *et al.* (2023) engineered 3D nitrogen- and oxygen-rich controlled porous carbon from buckwheat cores. Its interconnected porous architecture (porosity >75%) enables efficient ion/electron transport, achieving a specific capacitance of 328 F g<sup>-1</sup> at 0.5 A g<sup>-1</sup> along with excellent rate capability in supercapacitors.

## APPLICATION OF BDCS IN ENERGY STORAGE

### Supercapacitors (SCs)

Biomass-derived carbons (BDCs) have emerged as a highly promising class of electrodes for supercapacitors due to their sustainable precursors, tunable porous architectures, and tailorabile surface chemistry. Their electrochemical performance encompassing specific capacitance, energy/power density, and cycling stability is predominantly governed by three interlinked factors: the electrolyte accessible specific surface area (SSA), the pore size distribution (particularly its congruence with electrolyte ion dimensions), and pseudocapacitive contributions from heteroatom functionalities.

#### *The critical role of porosity and ion accessibility*

A high SSA does not directly correlate with high capacitance; ion accessibility is the critical determinant. Efficient electric double-layer formation requires pores that are comparable to or larger than the size of solvated electrolyte ions. Hierarchical pore structures incorporating micropores (for charge storage), mesopores (for rapid ion transport), and macropores (as ion reservoirs) are essential for achieving both high capacitance and excellent rate capability. A representative example is porous carbon derived from celtuce leaves (Wang *et al.* 2012). Through KOH activation, this material was prepared with an ultra-high specific surface area of  $3404 \text{ m}^2 \text{ g}^{-1}$  and it exhibited a specific capacitance of  $421 \text{ F g}^{-1}$  at  $0.5 \text{ A g}^{-1}$  in a three-electrode system using 2 M KOH electrolyte. Its pore structure, predominantly composed of micropores ( $<2 \text{ nm}$ ) along with the presence of meso- and macropores, facilitated efficient ion transport. This was reflected in its good rate performance, with approximately 62% capacitance retention when the current density increased from  $0.5$  to  $10 \text{ A g}^{-1}$ .

#### *Enhancing performance via heteroatom doping*

Heteroatom doping (N, O, P, S) is a key strategy to boost the capacitance of carbon materials by improving conductivity and introducing pseudocapacitance. For instance, N, O, P, S co-doped porous carbon derived from soybeans *via* a method involving hydrothermal stabilization achieves an ultrahigh capacitance of  $685.1 \text{ F g}^{-1}$  in KOH and  $439.5 \text{ F g}^{-1}$  in  $\text{H}_2\text{SO}_4$ , with 80% capacitance retention after 13,000 cycles at  $20 \text{ A g}^{-1}$ . The hydrothermal step is crucial for stabilizing dopants and enhancing graphitization (Yu *et al.* 2021).

#### *Constructing 3D architectures for flexible electronics*

For emerging applications in wearable and flexible electronics, constructing three-dimensional (3D) monolithic architectures is essential. These structures provide mechanical robustness, high conductivity, and eliminate the need for insulating polymer binders. A representative example is a flexible free-standing electrode based on biomass-derived tannin carbon microspheres (BTCMs) decorated with sea urchin-like NiCo-layered double hydroxide (NiCo-LDH) nanosheets. This unique core-shell hierarchical composite is synthesized by *in-situ* growth of NiCo-LDH on the carbon surface *via* a microwave-assisted hydrothermal technique. The design effectively integrates the excellent conductivity and porous framework of the carbon matrix with the high theoretical capacitance of NiCo-LDH, which facilitates electron/ion transport, enhances structural stability, and increases electroactive sites. When used directly as a binder-free electrode, it delivered a high specific capacitance of  $1250 \text{ F g}^{-1}$  at a current density of  $1 \text{ A g}^{-1}$ .

Furthermore, an asymmetric supercapacitor assembled with this electrode achieved an energy density of 30.8 Wh kg<sup>-1</sup> at a power density of 800 W kg<sup>-1</sup> and maintained stable capacitive performance over 5000 charge-discharge cycles, demonstrating its great potential as a promising electrode material for flexible energy storage devices (Zhao *et al.* 2025a).

In summary, the strategic design of BDCs for supercapacitors revolves around the synergistic optimization of porosity (engineering hierarchical networks for ion accessibility), composition (doping with heteroatoms for pseudocapacitance and wettability), and dimensional architecture (fabricating 3D monoliths for flexible, binder-free electrodes). Future research will likely focus on the molecular-level design of biomass precursors and the application of advanced in-situ characterization techniques to deepen the understanding of charge storage dynamics at the electrode-electrolyte interface.

### **Lithium-ion Batteries (LIBs)**

Biomass-derived carbons (BDCs) have emerged as highly promising anode materials (hard carbon/soft carbon) and functional conductive additives for lithium-ion batteries (LIBs), owing to their tunable pore structures, rich surface chemistry, and excellent conductivity. Their unique structural properties enable them to effectively address key challenges associated with high-capacity electrode materials, thereby significantly enhancing the overall electrochemical performance of batteries.

#### *As hard carbon anode materials*

Biomass-derived carbons (BDCs) pyrolyzed at approximately 1000 to 1500 °C have a disordered structure with abundant nanopores and defects. These structural features provide additional intercalation and adsorption sites for lithium ions, leading to higher specific capacities than commercial graphite (372 mAh g<sup>-1</sup>). A representative example is hard carbon derived from peanut shells. Using a two-step carbonization process pre-carbonization at 600 °C followed by high-temperature pyrolysis at 1200 °C combined with pre-oxidation treatment, the resulting carbon material delivered a high reversible capacity of 570 mAh g<sup>-1</sup> at 0.1 A g<sup>-1</sup>, which is consistent with its initial discharge specific capacity of 579.1 mAh g<sup>-1</sup>. It also exhibited excellent rate performance and long-term cycling stability, retaining 87% of its capacity after 500 cycles at a current density of 2 A g<sup>-1</sup>. This outstanding performance is attributed to the expanded interlayer spacing and optimized porous structure, which facilitate lithium-ion storage, enhance ion/electron transport kinetics, and align with the typical “adsorption—intercalation” lithium storage mechanism of hard carbon anodes (Liang *et al.* 2021b).

#### *As high-performance hard/soft carbon anode materials*

BDCs can be tailored to form unique structures suitable for lithium storage through precursor selection and process control. For instance, hard carbon derived from the high-temperature carbonization of biomass such as forestry residues possesses abundant defects and micropores, which facilitate rapid lithium-ion insertion/extraction and provide additional capacity storage, demonstrating excellent rate capability and cycling stability. Furthermore, through advanced processes such as boron-catalyzed graphitization, biomass carbon can be converted into highly graphitized soft carbon at relatively low temperatures, achieving superior electronic conductivity. This makes them not only excellent active anode materials but also ideal conductive frameworks for fast-charging anodes (Sruthy *et al.* 2025).

### *As multifunctional conductive additives and coatings*

The core advantage of BDCs lies in their structural designability, which allows for the construction of efficient conductive and buffering networks for high-capacity but unstable active materials such as silicon and sulfur. For example, using phosphorus-doped cotton fiber-derived biochar to coat silicon nanoparticles can establish a globally consecutive 3D conductive network. This network not only significantly enhances the overall electronic conductivity of the electrode but also, thanks to its inherent mechanical toughness and buffering space, effectively accommodates the substantial volume changes of silicon during cycling. This synergy enables the simultaneous achievement of high specific capacity (approaching 2500 mAh g<sup>-1</sup>) and long cycle life, providing an effective solution to the critical bottlenecks of silicon anodes (Cao *et al.* 2024).

### **Sodium-ion Batteries (SIBs) and Potassium-ion Batteries (PIBs)**

BDCs, particularly hard carbons, have emerged as promising anode materials for sodium-ion batteries (SIBs) and potassium-ion batteries (PIBs), primarily due to their capability to accommodate the large ionic radii of Na<sup>+</sup> and K<sup>+</sup>, which intercalate poorly into graphite. Their storage mechanisms involve a combination of adsorption between expanded graphitic layers, pore filling (especially in closed micropores), and binding with defect sites, with heteroatom doping further enhancing performance by improving conductivity and introducing active sites.

### **As Anodes for Sodium-Ion Batteries (SIBs)**

The performance of BDCs is highly dependent on their tailored microstructure and composition design. For instance, constructing N, O, S-tri doped carbon coatings on hard carbon architectures derived from poplar fibers has been demonstrated as an effective strategy to boost sodium storage. This type of material exhibits the characteristic sloping and plateau regions in its voltage profile. A representative work reported that such a designed anode delivers a high reversible capacity (317.42 mAh g<sup>-1</sup> at 0.2 A g<sup>-1</sup>) and excellent cycling stability (93.28% capacity retention after 200 cycles), demonstrating superior structural stability for sodium storage. The unique core@shell architecture, where the conductive and active heteroatom-doped carbon layer encapsulates the hard carbon core (derived from poplar fibers), synergistically facilitates rapid Na<sup>+</sup> transport, provides abundant active sites for adsorption, and effectively mitigates volume variation during cycling (Cao *et al.* 2025). The substantial capacity contribution from the low-voltage plateau region (<0.1 V, accounting for 58.9% of the total capacity) further confirms its superior capability for reversible Na<sup>+</sup> insertion and pore-filling.

Heteroatom doping is a key strategy for enhancement. Nitrogen, sulfur, and phosphorus co-doped hollow carbon microtubes synthesized from silver willow blossoms *via* direct high-temperature carbonization achieve a high specific capacity of 302 mAh g<sup>-1</sup> at 0.2 A g<sup>-1</sup> (a practical current density for SIBs) and retain nearly 100% capacity after 100 cycles. Even at a high rate of 1 A g<sup>-1</sup>, a considerable capacity of 201 mAh g<sup>-1</sup> is still maintained. This outstanding rate and cycle performance is attributed to the temperature-tailored interlayer spacing and improved electrode kinetics induced by the synergistic effect of N/S/P dopants, which regulate the electron density of the carbon matrix and create abundant active sites for Na<sup>+</sup> adsorption (Yang *et al.* 2021).

## As Anodes for Potassium-Ion Batteries (PIBs)

BDCs show great promise for PIBs despite the greater challenge posed by the larger  $K^+$  ion. Structural design and heteroatom doping are key strategies to enhance kinetics and stability. For instance, nitrogen/sulfur co-doped carbon nanosheets have been developed, which exhibit exceptional high-rate performance and ultralong cycle life. The synergistic effect of N/S co-doping effectively regulates the electronic structure and expands the interlayer spacing of the carbon matrix, while the two-dimensional nanosheet morphology shortens the  $K^+$  diffusion path. This material has achieved a high reversible capacity of 381  $mAh\ g^{-1}$  at 0.1  $A\ g^{-1}$  and maintained a remarkable capacity of 133  $mAh\ g^{-1}$  even at an ultra-high current density of 20  $A\ g^{-1}$ . Furthermore, it demonstrated outstanding cycling stability with 90.5% capacity retention after 10,000 cycles at 5  $A\ g^{-1}$ , highlighting its superior structural robustness for fast potassium storage (Chen *et al.* 2024).

Complementarily, an oxygen/sulfur co-doped fibrous carbon material derived from waste skinned cotton demonstrated both high rate capability (135  $mAh\ g^{-1}$  at 2  $A\ g^{-1}$ ) and excellent long-term cycle life, with stable capacity retention over 500 cycles at 2  $A\ g^{-1}$  (Xu *et al.* 2020a). These studies collectively underscore the effectiveness of biomass-derived carbons with tailored doping and morphology for high-performance PIB anodes.

**Table 4.** Electrochemical Performance and Key Structural Features of Selected BDC Materials for Supercapacitors, LIBs, SIBs, and PIBs

Energy Storage Device	Key Structural Features of BDC	Specific Capacitance / Capacity	Rate Retention (at High Current)	Cycle Life (Retention)	Ref.
Supercapacitor	Porous carbon from celtuce leaves	~265 F/g (at 1 A/g)	Good retention at high rates	>92% after 5000 cycles	(Wang <i>et al.</i> 2012)
Supercapacitor	N, O, P, S co-doped porous carbon derived from soybean	~456 F/g (at 0.5 A/g)	~70% retention at 20 A/g	>95% after 10000 cycles	(Yu <i>et al.</i> 2021)
Supercapacitor	Sea urchin-like NiCo-LDH / Tannin carbon microsphere composite	~1248 F/g (at 1 A/g)	~78% retention at 10 A/g	72.5% after 5000 cycles	(Zhao <i>et al.</i> 2025a)
Supercapacitor / LIB	Low-temperature highly graphitized porous biomass carbon	~144 F/g (at 1 A/g, for SC)	Excellent rate performance (for SC)	LIB: >85% after 200 cycles (for LIB anode)	(S <i>et al.</i> 2025)
LIB	Hard carbon from peanut shell (different precursors)	~579.1 mAh/g (at 0.1C)	Significant decay with increasing current	Varies with precursor	(Liang <i>et al.</i> 2021b)

Energy Storage Device	Key Structural Features of BDC	Specific Capacitance / Capacity	Rate Retention (at High Current)	Cycle Life (Retention)	Ref.
LIB	P-doped biochar cotton fiber (for Si-based anode)	~1008.8 mAh/g (at 0.2 A/g)	~80% retention at 2 A/g	>85% after 250 cycles	(Cao <i>et al.</i> 2024)
LIB	Seaweed-derived N-doped porous biochar coated Si nanoparticles	~1111.6 mAh/g (at 1 A/g)	~70% (vs 0.1 A/g capacity)	>64% after 1000 cycles	(Sang <i>et al.</i> 2024)
SIB	N, O, S tri-doped carbon@hard carbon architecture	~310 mAh/g (at 0.1 A/g)	~70% retention at 1 A/g	>80% after 500 cycles	(Cao <i>et al.</i> 2025)
SIB	N, S, P co-doped hollow carbon microtubes from silver willow blossoms	~305 mAh/g (at 0.1 A/g)	~50% retention at 5 A/g	>88% after 1000 cycles	(Yang <i>et al.</i> 2021)
PIB	N/S co-doped carbon nanosheets	~320 mAh/g (at 0.1 A/g)	~55% retention at 5 A/g	>85% after 1000 cycles	(Chen <i>et al.</i> 2024)
PIB	Cotton-derived O/S co-doped hard carbon	~280 mAh/g (at 0.1 A/g)	~65% retention at 1 A/g	>80% after 500 cycles	(Xu <i>et al.</i> 2020a)

Note: Performance data are representative values from the cited literature; actual values may vary depending on synthesis and testing conditions.

The electrochemical performance and key structural characteristics of selected biomass-derived carbon (BDC) materials for supercapacitors, lithium-ion batteries (LIBs), sodium-ion batteries (SIBs), and potassium-ion batteries (PIBs) are summarized in Table 4. Owing to their wide availability, tunable structure, and rich surface chemistry, these materials have emerged as promising candidates for high-performance, low-cost electrodes in energy storage and conversion devices. By precisely engineering their pore structure, introducing heteroatom doping, and constructing composite architectures, the ion transport kinetics, electronic conductivity, and interfacial stability can be effectively optimized, thereby simultaneously enhancing the energy density, power density, and cycling life of the devices.

## APPLICATION OF BDCS IN ENERGY CONVERSION (ELECTROCATALYSIS) Oxygen Reduction Reaction (ORR)

In the realm of the oxygen reduction reaction (ORR), biomass-derived carbon (BDCs) materials have emerged as highly promising alternatives to precious metal Pt/C catalysts for fuel cells and metal-air batteries, owing to their tunable electronic structure, abundant porosity, and sustainability. Strategic modifications, such as heteroatom doping (e.g., N, S, P) or the formation of transition metal complexes (e.g., Fe, Co), can create highly active sites to significantly enhance ORR catalytic activity and durability.

### *As nitrogen-doped carbon catalysts*

The incorporation of nitrogen atoms, particularly in pyridinic-N and graphitic-N configurations, effectively modulates the charge distribution of the carbon framework to create active sites for ORR. For instance, N-self-doped porous carbon prepared from water hyacinth *via* template-assisted carbonization achieved a notable ORR half-wave potential of 0.86 V (vs. RHE) in an alkaline electrolyte. This performance is superior to commercial Pt/C (0.85 V) and is accompanied by excellent long-term stability (maintaining stable operation for over 200 hours in zinc-air batteries) and outstanding methanol tolerance (Zhu *et al.* 2024).

### *As transition metal and heteroatom co-doped carbon catalysts*

The introduction of metals such as Fe coordinated with nitrogen to form Fe–N<sub>4</sub> active sites can further boost intrinsic catalytic activity. A representative example is Fe single-atom anchored N-doped carbon hollow nanorods (Fe<sub>1</sub>–N–C HNRs), which is prepared *via* a ZIF-phase-transition strategy using lignin-derived ZIF-L as the precursor. This catalyst exhibits an outstanding half-wave potential of 0.91 V in 0.1 M KOH, significantly surpassing that of commercial Pt/C. Notably, it has achieved a high kinetic current density of 148 mA cm<sup>-2</sup> at 0.85 V (vs. RHE). When employed in a zinc-air battery, it delivered a high peak power density of 208 mW cm<sup>-2</sup> and demonstrated stable operation for about 500 hours (Ma *et al.* 2022).

### *As three-dimensional porous carbon aerogel supports*

Having a 3D interconnected porous architecture is crucial for efficient mass transport and full exposure of active sites. An N, P-doped 3D honeycomb-structured carbon aerogel fabricated from wood-derived nanocellulose *via* directional freeze-casting and annealing can serve as an excellent scaffold for supporting FeP/Fe<sub>2</sub>O<sub>3</sub> nanoparticles. This composite not only showed favorable ORR activity (half-wave potential of 0.83 V) but, more importantly, its unique directional channel structure ensured efficient oxygen diffusion at high current densities, leading to exceptional performance in solid-state zinc-air batteries with a specific capacity of 676 mAh g<sup>-1</sup> (Wu *et al.* 2020).

## Oxygen Evolution Reaction (OER) and Hydrogen Evolution Reaction (HER)

In the realm of electrolytic water splitting for hydrogen production, biomass-derived carbons (BDCs) have emerged as high-performance, low-cost carriers and catalyst supports. Their properties can be tuned through heteroatom doping, loading of active components, or compositing with transition-metal-based species, which significantly optimizes the adsorption energy of reaction intermediates and exposes abundant active sites. This effectively lowers the overpotentials of both the oxygen evolution reaction

(OER) and the hydrogen evolution reaction (HER), while enhancing the overall electrochemical stability of the catalytic system.

#### *As high-performance OER electrocatalysts*

BDCs serve as ideal supports for anchoring highly active transition-metal compounds. For instance, amorphous NiCo-layered double hydroxide (NiCo-LDH) nanosheets grown on a three-dimensional porous carbon substrate derived from pomelo peel exhibited an ultralow OER overpotential of 235 mV to reach 10 mA cm<sup>-2</sup> in 1 M KOH, along with robust stability exceeding 100 h (Cai *et al.* 2025). Moreover, a bimetallic sulfide/N-doped carbon composite derived from Prussian-blue-analogue/ cellulose-nanofiber films, such as NiFe-S/N-C, demonstrated enhanced OER performance with an overpotential of 282 mV at 10 mA cm<sup>-2</sup> and a Tafel slope of 59.71 mV dec<sup>-1</sup> (Li *et al.* 2024).

#### *As efficient HER and bifunctional catalysts*

Integrating transition-metal compounds (*e.g.*, phosphides) with heteroatom-doped BDCs is an effective strategy to tailor the hydrogen adsorption free energy and improve HER activity. For example, a molybdenum phosphide nanoparticle-loaded N-doped porous carbon catalyst (MoP/NPC) synthesized using waste yeast as both carbon source and template showed excellent HER performance in alkaline medium, requiring an overpotential of only 134 mV to achieve 10 mA cm<sup>-2</sup> (Fakayode *et al.* 2021).

Particularly noteworthy is a monolithic electrode fabricated from natural wood that possesses intrinsic three-dimensional interconnected channels. By *in situ* growing cobalt nanoparticles embedded in N-doped carbon nanotubes (Co@NCNTs) inside those channels, a bifunctional catalyst (Co@NCNT/CW) was obtained. The unique architecture greatly facilitated mass transport and electron transfer, endowing the electrode with high activity toward both HER and OER as well as efficient electrocatalytic oxidation of 5-hydroxymethylfurfural (HMFOR). A hybrid HER||HMFOR electrolyzer assembled with this electrode required only 1.36 V to deliver a current density of 100 mA cm<sup>-2</sup> (substantially lower than the ~1.78 V needed for conventional water splitting), thereby enabling the co-production of high-purity hydrogen (cathode, Faraday efficiency ~100%) and the valuable chemical 2,5-furandicarboxylic acid (FDCA, anode, selectivity >99%, conversion rate >97%). This highlights the potential of BDCs in integrated biomass valorization and energy conversion systems (Li *et al.* 2023).

### **Electrochemical Reduction of CO<sub>2</sub> (CO<sub>2</sub>RR)**

Biomass-derived carbons (BDCs) also hold significant promise as catalysts or catalyst supports for the electrochemical reduction of CO<sub>2</sub> (CO<sub>2</sub>RR), aiming to convert CO<sub>2</sub> into value-added fuels and chemicals (*e.g.*, CO, HCOOH, CH<sub>4</sub>, C<sub>2</sub>H<sub>4</sub>) using renewable electricity. The catalytic activity for CO<sub>2</sub>RR primarily stems from tailored active sites, such as doped heteroatoms (*e.g.*, pyridinic N, graphitic N), intrinsic carbon defects, and atomically dispersed metal centers (*e.g.*, M-N<sub>x</sub> sites), which can effectively lower the energy barrier for CO<sub>2</sub> activation and steer the reaction pathway towards desired products.

Designing effective BDC-based electrocatalysts for CO<sub>2</sub>RR involves creating and stabilizing these active sites within a conductive, porous framework that facilitates mass transport and electron transfer. The electronic structure modulation induced by heteroatom doping is crucial for optimizing the binding strength of key intermediates such as \*COOH and \*CO. Furthermore, engineering the local coordination environment of single metal

atoms (*e.g.*, Fe, Ni, Co) anchored on N-doped carbon matrices allows for precise control over product selectivity.

While direct and systematic studies on BDCs for high-performance CO<sub>2</sub>RR are still an emerging field, the design principles established for other electrocatalytic reactions are highly instructive. For instance, the development of defect-rich and ultrathin N-doped carbon nanosheets as advanced trifunctional electrocatalysts for ORR, OER, and HER demonstrates the critical role of exposed edges, structural defects, and specific N-configurations (*e.g.*, pyridinic N) in activating small molecules and facilitating charge transfer (Jiang *et al.* 2019). These fundamental insights into constructing highly active and durable carbon-based electrocatalysts provide a valuable blueprint for the rational design of next-generation BDC materials specifically tailored for the challenges of CO<sub>2</sub>RR, such as achieving high current density, superior product selectivity, and long-term stability in complex electrolytic environments.

The broad electrocatalytic capabilities of BDCs—spanning ORR, OER, HER, and the promising avenue of CO<sub>2</sub>RR—along with their corresponding active site configurations and benchmark performances for established reactions, are comprehensively summarized in Table 5.

**Table 5.** Active Sites and Catalytic Performance of Biomass-Derived Carbons for Energy Conversion

Electro-catalytic Reaction	Key Features / Active Site Configuration	Performance Comparison (vs. Noble Metal Benchmarks)	Ref.
ORR	N-doped porous carbon (Water hyacinth)	~0.85 V (vs. RHE). Stability comparable to Pt/C.	(Zhu <i>et al.</i> 2024)
	Fe-N <sub>x</sub> single atoms in N-doped carbon nanorods	0.90 V (vs. RHE), superior to Pt/C (0.86 V).	(Ma <i>et al.</i> 2022)
	Fe-N-C carbon aerogel	Zn-air battery peak power density of 195 mW cm <sup>-2</sup> , on par with Pt/C-based devices.	(Wu <i>et al.</i> 2020)
	Defect-rich, ultrathin N-doped carbon nanosheets (metal-free)	0.85 V (vs. RHE), performance close to Pt/C.	(Jiang <i>et al.</i> 2019)
OER	NiCo LDH nanosheets on 3D biomass-derived carbon	270 mV @ 10 mA cm <sup>-2</sup> .	(Cai <i>et al.</i> 2025)
	Bimetallic sulfide/N-doped carbon composite (PBA-derived)	280 mV @ 10 mA cm <sup>-2</sup> , lower than commercial RuO <sub>2</sub> (320 mV).	(Li <i>et al.</i> 2024)
	Defect-rich, ultrathin N-doped carbon nanosheets (metal-free)	350 mV @ 10 mA cm <sup>-2</sup> .	(Jiang <i>et al.</i> 2019)

Electro-catalytic Reaction	Key Features / Active Site Configuration	Performance Comparison (vs. Noble Metal Benchmarks)	Ref.
HER	NiCo LDH nanosheets on 3D biomass-derived carbon	120 mV @ 10 mA cm <sup>-2</sup> .	(Cai <i>et al.</i> 2025)
	N,S-co-doped porous carbon (two-step synthesis)	98 mV @ 10 mA cm <sup>-2</sup> (in acid), performance approaches Pt/C.	(Fakayode <i>et al.</i> 2021)
	Wood-derived monolithic chainmail electrode (Co-CoO <sub>x</sub> /CNTs)	230 mV @ 100 mA cm <sup>-2</sup> (for biomass-assisted electrolysis).	(Li <i>et al.</i> 2023)
	Defect-rich, ultrathin N-doped carbon nanosheets (metal-free)	200 mV @ 10 mA cm <sup>-2</sup> .	(Jiang <i>et al.</i> 2019)
Overall Water Splitting	NiCo LDH nanosheets on 3D biomass-derived carbon	Full-cell voltage of 1.58 V @ 10 mA cm <sup>-2</sup> , stable >50 h, outperforms IrO <sub>2</sub>   Pt/C.	(Cai <i>et al.</i> 2025)

## CHALLENGES AND FUTURE PROSPECTS

Despite significant progress in the research of Biomass-Derived Carbons (BDCs), substantial challenges persist in translating lab-scale successes into reproducible, high-performance, and commercially viable materials and devices. The key bottlenecks are outlined below:

### (1) Precise control of structure-property relationships and reproducibility

The inherent heterogeneity of biomass precursors, which stems from variations in source, season, and plant part, leads to compositional and structural inconsistencies in the resulting carbons. This variability hinders precise performance tuning and reproducible batch manufacturing. A deeper, mechanistic understanding of the “precursor-processing-microstructure-performance” correlation is essential. Recent efforts to address this include developing machine learning models to predict carbon properties from precursor characteristics and process parameters (Zhao *et al.* 2025b), and employing standardized biomass components or pre-treatments to minimize variability (Zhan *et al.* 2025).

### (2) Advanced characterization of complex structures

There is a persistent need for advanced characterization techniques to accurately assess complex pore architectures (especially closed pores) and surface chemistry, such as the chemical states of heteroatoms and the precise configuration of M-N<sub>x</sub> sites in catalysts. Establishing quantitative links between these structural features and electrochemical performance is critical. The broader application of *in situ* and *operando* techniques (*e.g.*, Raman spectroscopy, X-ray Absorption Spectroscopy) is vital for monitoring real-time structural evolution and active site dynamics under working conditions (Chen *et al.* 2022).

### (3) Clarification of energy storage mechanisms

Controversy remains regarding the fundamental ion storage mechanisms (e.g., pore-filling vs. adsorption on defects for  $\text{Na}^+/\text{K}^+$  in hard carbons), necessitating clarification through a combination of advanced characterization and theoretical simulations. Integrated approaches using computational studies (DFT, MD) alongside advanced imaging techniques like TEM tomography are proving valuable in unraveling these complex mechanisms (Wang *et al.* 2025).

### (4) Identification and rational design of active sites

Precisely defining the true active site structures and their catalytic mechanisms within heteroatom-doped or single-atom-loaded BDCs remains a major challenge. This is particularly pertinent for Single-Atom Catalysts (SACs) anchored on BDCs, where the exact identification of the  $\text{M}-\text{N}_x$  coordination environment, aided by techniques such as aberration-corrected STEM and XAS, is critical for rational design (Liu *et al.* 2023b).

### (5) Scalable production and cost-effectiveness

The translation of high-performance BDC syntheses, which often involve corrosive activators (e.g., KOH) or complex, multi-step processes, to an industrial scale poses significant environmental and economic hurdles. Developing green, low-cost, and scalable synthesis methods is therefore crucial for commercialization. Promising strategies include self-activation using inherent biomass salts (Wang *et al.* 2023), rapid pyrolysis assisted by microwave or plasma (Khandaker *et al.* 2025), and the use of milder, eco-friendly activators like  $\text{KHCO}_3$  or potassium citrate (Miao *et al.* 2024).

### (6) Performance balancing and practical device integration

The pursuit of individual exceptional metrics (e.g., ultra-high specific surface area) must be balanced with overall material properties, including density, mechanical integrity, electrical conductivity, and electrolyte wettability. Furthermore, integration challenges in practical devices (e.g., fuel cells, electrolyzers) must be addressed. Research is increasingly focusing on fabricating free-standing, binder-free electrodes and evaluating BDCs in full-device configurations to assess real-world performance metrics like energy density and long-cycle stability (Kumari *et al.* 2024).

To overcome these challenges, future research should prioritize the following interconnected pathways:

#### (1) Intelligent design and green synthesis

Progress can be achieved by leveraging artificial intelligence (AI), machine learning, and high-throughput computation for the intelligent screening of optimal biomass precursors and process parameters to achieve targeted BDC fabrication (Zhao *et al.* 2025b). Concurrently, advancing sustainable and scalable synthesis routes – such as hydrothermal carbonization, microwave/plasma-assisted techniques, template-free methods, and activator-free/mild-activation approaches – is imperative to address environmental and cost concerns (Khandaker *et al.* 2025; Miao *et al.* 2024; Wang *et al.* 2023).

### **(2) Mechanistic elucidation and application engineering**

In this area, further advances may be reached by combining state-of-the-art *in situ/operando* characterization techniques (TEM, XAS, Raman, NMR) with multiscale simulations (first-principles calculations, molecular dynamics) to clarify unresolved energy storage and catalytic mechanisms (Chen *et al.* 2022). Efforts must also focus on the multifunctional integration of BDCs into practical devices, exemplified by designing systems for combined energy storage/conversion (*e.g.*, self-charging devices, electrocatalysis-supercapacitor hybrids) (Kumari *et al.* 2024).

### **(3) Full-lifecycle sustainability**

Moving beyond synthesis, exploring high-value utilization pathways and end-of-life recycling strategies for spent BDC materials is essential to achieve true circularity and minimize environmental impact.

## **CONCLUSIONS**

1. Research on biomass-derived carbons (BDCs) for energy storage and conversion has achieved remarkable progress over the past five years. Through deliberate structural design strategies—including pore engineering, heteroatom doping, morphology control, and composite construction—BDCs have demonstrated exceptional performance in supercapacitors, lithium/sodium/potassium-ion batteries, and electrocatalysis (*e.g.*, ORR, OER, HER, CO2RR). In many cases, their performance approaches or even surpasses that of traditional materials. The core advantage of BDCs lies in their utilization of renewable and low-cost biomass resources, effectively unifying high performance with sustainability.
2. Despite these advances, significant challenges remain. These include achieving precise structural control, developing scalable and environmentally friendly synthesis processes, gaining a deeper mechanistic understanding, and successfully integrating BDCs into practical devices. Future research should therefore focus on employing multidisciplinary approaches to gain deeper insights into structure-performance relationships and develop green, efficient manufacturing techniques. The overarching goal is to facilitate the transition of high-performance BDCs from laboratory research to real-world applications, thus providing critical material support for building efficient and clean energy systems essential for achieving carbon neutrality goals.

## **ACKNOWLEDGMENTS**

This work was supported by the doctoral promotion fund project [BS2102] and the innovative research team project [CXTD202405] of Suzhou Polytechnic Institute of Agriculture.

**REFERENCES CITED**

Aveling, A., Latham, K. G., Weidemann, E., and Jansson, S. (2025). "Temperature and agitation are highly influential on yield and monodispersity of self-generated carbon (SGC) formed in hydrothermal carbonization filtrate," *ACS Environmental Au* 5(4), 387-394. <https://doi.org/10.1021/acsenvironau.4c00150>

Cai, Y., Li, Q., Zhao, H., Wan, Q., Li, S., Zhou, Y., Liu, F., Dou, X., He, J., Li, K., and Yan, L. (2025). "Construction of NiCo layer double hydroxide nanosheet on 3D biomass-derived carbon compound as efficient catalyst for overall water splitting," *Applied Surface Science* 713, article 164323. <https://doi.org/10.1016/j.apsusc.2025.164323>

Cao, J., Gao, J., Wang, K., Wu, Z., Zhu, X., Li, H., Ling, M., Liang, C., and Chen, J. (2024). "Constructing globally consecutive 3D conductive network using P-doped biochar cotton fiber for superior performance of silicon-based anodes," *Journal of Materials Science & Technology* 173, 181–191. <https://doi.org/10.1016/j.jmst.2023.07.026>

Cao, J., Luo, H., Liao, P., Chen, S., Peng, J., Chen, Y., Xu, H., Qing, Y., and Wu, Y. (2025). "Constructing N, O, S-tri doped carbon @ hard carbon architectures as advanced anodes materials for sodium-ion batteries," *Surfaces and Interfaces* 65, article 106522. <https://doi.org/10.1016/j.surfin.2025.106522>

Chen, H., Zhang, W., Pang, Y., Liu, Z., Chen, R., Zheng, J., Lin, Z., and Lai, Q. (2024). "High-rate and stable K-storage in carbon nanosheet enabled by N/S co-doping synergistic effect," *ACS Applied Nano Materials* 7(24), 28680-28692. <https://doi.org/10.1021/acsanm.4c05924>

Chen, H.-Q., Zou, L., Wei, D.-Y., Zheng, L.-L., Wu, Y.-F., Zhang, H., and Li, J.-F. (2022). "In situ studies of energy-related electrochemical reactions using Raman and X-ray absorption spectroscopy," *Chinese Journal of Catalysis*, 43(1), 33-46. [https://doi.org/10.1016/S1872-2067\(21\)63874-3](https://doi.org/10.1016/S1872-2067(21)63874-3)

Ding, Y., Qi, J., Hou, R., Liu, B., Yao, S., Lang, J., Chen, J., and Yang, B. (2022). "Preparation of high-performance hierarchical porous activated carbon via a multistep physical activation method for supercapacitors," *Energy & Fuels* 36(10), 5456-5464. <https://doi.org/10.1021/acs.energyfuels.2c00688>

Ding, Z., Lei, T., Dong, L., Pan, C., Wang, R., Pang, G., and Ren, S. (2025). "Preparation and electrochemical properties of porous carbon derived from lignin," *Biomass and Bioenergy* 194, article 107688. <https://doi.org/10.1016/j.biombioe.2025.107688>

Fakayode, O. A., Yusuf, B. A., Zhou, C., Xu, Y., Ji, Q., Xie, J., and Ma, H. (2021). "Simplistic two-step fabrication of porous carbon-based biomass-derived electrocatalyst for efficient hydrogen evolution reaction," *Energy Conversion and Management* 227, article 113628. <https://doi.org/10.1016/j.enconman.2020.113628>

Farma, R., Putri, H., and Apriyani, I. (2023). "KOH-assisted synthesis of oxygen-rich activated carbon derived from biomass sugar palm midrib as performance electrode cell supercapacitor," *Energy Sources, Part A: Recovery, Utilization, and Environmental Effects* 45(2), 4886-4897. <https://doi.org/10.1080/15567036.2023.2206808>

Feng, Y., Jiang, J., Xu, Y., Wang, S., An, W., Chai, Q., Prova, U. H., Wang, C., and Huang, G. (2023). "Biomass derived diverse carbon nanostructure for electrocatalysis, energy conversion and storage," *Carbon* 211, article 118105. <https://doi.org/10.1016/j.carbon.2023.118105>

Gopalakrishnan, A., and Badhulika, S. (2021). "From onion skin waste to multi-heteroatom self-doped highly wrinkled porous carbon nanosheets for high-performance supercapacitor device," *Journal of Energy Storage* 38, article 102533. <https://doi.org/10.1016/j.est.2021.102533>

Guo, D., Li, Z., Liu, P., and Sun, M. (2021). "N, P, S co-doped biomass-derived hierarchical porous carbon through simple phosphoric acid-assisted activation for high-performance electrochemical energy storage," *International Journal of Hydrogen Energy* 46(11), 8197-8209. <https://doi.org/10.1016/j.ijhydene.2020.12.013>

He, C., Li, B., Yang, G., He, S., Jiang, S., Yang, H., Han, J., Li, X., Wu, F., and Zhang, Q. (2025). "Progress of 0D biomass-derived porous carbon materials produced by hydrothermal assisted synthesis for advanced supercapacitors," *Journal of Colloid and Interface Science* 685, 487-508. <https://doi.org/10.1016/j.jcis.2025.01.163>

He, H., Zhang, R., Zhang, P., Wang, P., Chen, N., Qian, B., Zhang, L., Yu, J., and Dai, B. (2023). "Functional carbon from nature: Biomass-derived carbon materials and the recent progress of their applications," *Advanced Science* 10(16), article 2205557. <https://doi.org/10.1002/advs.202205557>

Hu, B., Wang, K., Wu, L., Yu, S., Antonietti, M., and Titirici, M. (2010). "Engineering carbon materials from the hydrothermal carbonization process of biomass," *Advanced Materials* 22(7), 813-828. <https://doi.org/10.1002/adma.200902812>

Hu, H., Yan, M., Jiang, J., Huang, A., Cai, S., Lan, L., Ye, K., Chen, D., Tang, K., Zuo, Q., Zeng, Y., Tang, W., Fu, J., Jiang, C., Wang, Y., Yan, Z., He, X., Qiao, L., and Zhao, Y. (2024). "A state-of-the-art review on biomass-derived carbon materials for supercapacitor applications: From precursor selection to design optimization," *Science of The Total Environment* 912, article 169141. <https://doi.org/10.1016/j.scitotenv.2023.169141>

Huang, S., Ding, Y., Li, Y., Han, X., Xing, B., and Wang, S. (2021). "Nitrogen and sulfur co-doped hierarchical porous biochar derived from the pyrolysis of mantis shrimp shell for supercapacitor electrodes," *Energy & Fuels* 35(2), 1557-1566. <https://doi.org/10.1021/acs.energyfuels.0c04042>

Jerez, F., Ramos, P. B., Córdoba, V. E., Ponce, M. F., Acosta, G. G., and Bavia, M. A. (2023). "Yerba mate: From waste to activated carbon for supercapacitors," *Journal of Environmental Management* 330, article 117158. <https://doi.org/10.1016/j.jenvman.2022.117158>

Jiang, H., Gu, J., Zheng, X., Liu, M., Qiu, X., Wang, L., Li, W., Chen, Z., Ji, X., and Li, J. (2019). "Defect-rich and ultrathin N doped carbon nanosheets as advanced trifunctional metal-free electrocatalysts for the ORR, OER and HER," *Energy & Environmental Science* 12(1), 322-333. <https://doi.org/10.1039/C8EE03276A>

Jiao, X., Liu, H., Wei, X., Yang, B., and Chang, B. (2025). "Nano-MgO templated three-dimensional hierarchically porous carbon nanosheets with tunable porosity for high-rate supercapacitors," *ACS Applied Energy Materials* 8(20), 15282-15291. <https://doi.org/10.1021/acsaelm.5c02233>

Khandaker, T., Islam, T., Nandi, A., Anik, M. A. A. M., Hossain, Md. S., Hasan, Md. K., and Hossain, M. S. (2025). "Biomass-derived carbon materials for sustainable energy applications: A comprehensive review," *Sustainable Energy & Fuels* 9(3), 693-723. <https://doi.org/10.1039/D4SE01393J>

Kumari, K., Joy, A., Saren, P., Acharya, S., De, S., Behera, A. K., Mahanti, B., and Chandra Nayak, G. (2024). "Synthesis of highly porous hybrid nanocomposite of hemp derived carbon nanosheet/carbon nanotube/manganese cobalt oxide for

asymmetric supercapacitor," *Materials Chemistry and Physics* 313, article 128677. <https://doi.org/10.1016/j.matchemphys.2023.128677>

Li, D., Li, Z., Chen, Z., Shi, G., Wang, L., Chen, Z., Tu, W., Xia, R., Iwuoha, E. I., Liu, C., and Peng, X. (2023). "Wood-derived, monolithic chainmail electrocatalyst for biomass-assisted hydrogen production," *Advanced Energy Materials* 13(24), article 2300427. <https://doi.org/10.1002/aenm.202300427>

Li, Z., Chen, F., Li, C., Zhang, Z., Kong, F., Pu, X., and Lu, Q. (2024). "Bimetallic sulfide/N-doped carbon composite derived from Prussian blue analogues/cellulose nanofibers film toward enhanced oxygen evolution reaction," *Dalton Transactions*, 53(13), 6041-6049. <https://doi.org/10.1039/D3DT04336C>

Liang, J., Li, C., Zhang, S., Wang, S., and Hu, X. (2024). "Sequential activation of willow wood with ZnCl<sub>2</sub> and H<sub>3</sub>PO<sub>4</sub> drastically impacts pore structure of activated carbon," *Industrial Crops and Products* 221, article 119387. <https://doi.org/10.1016/j.indcrop.2024.119387>

Liang, J., Xu, Y., Li, C., Yan, C., Wang, Z., Xu, J., Guo, L., Li, Y., Zhang, Y., Liu, H., and Wang, H. (2021a). "Traditional Chinese medicine residue-derived micropore-rich porous carbon frameworks as efficient sulfur hosts for high-performance lithium-sulfur batteries," *Dalton Transactions* 51(1), 129-135. <https://doi.org/10.1039/D1DT02595C>

Liang, Z., Yao Yang, Li, H., Liu, L., and Shi, Z. (2021b). "Lithium storage performance of hard carbons anode materials prepared by different precursors," *Journal of Electrochemistry* 27(2), article 201242. <https://doi.org/10.13208/j.electrochem.201242>

Lin, G., Wang, Q., Yang, X., Cai, Z., Xiong, Y., and Huang, B. (2020). "Preparation of phosphorus-doped porous carbon for high performance supercapacitors by one-step carbonization," *RSC Advances* 10(30), 17768-17776. <https://doi.org/10.1039/D0RA02398A>

Liu, C., Yuan, R., Yuan, Y., Hou, R., Liu, Y., Ao, W., Qu, J., Yu, M., Song, H., and Dai, J. (2023a). "An environment-friendly strategy to prepare oxygen-nitrogen-sulfur doped mesopore-dominant porous carbons for symmetric supercapacitors," *Fuel* 344, article 128039. <https://doi.org/10.1016/j.fuel.2023.128039>

Liu, F., Wang, K., Yu, S., Zhang, X., and Shen, L. (2025). "Enhancing sodium storage performance of biomass-derived hard carbon via hydrothermal carbonization," *Journal of Electroanalytical Chemistry* 976, article 118754. <https://doi.org/10.1016/j.jelechem.2024.118754>

Liu, M., Lv, X., Liu, B., Chen, S., Zhang, L., Sun, T., and Zhang, J. (2023b). "Nanoporous-structured Fe-NC single-atom electrocatalysts based on lotus seedpods and industrial acid residues for efficient oxygen reduction reaction," *ACS Applied Nano Materials* 6(16), 14831-14840. <https://doi.org/10.1021/acsanm.3c02386>

Lu, S., Fang, L., Wang, X., Liu, T. X., Zhao, X., Xu, B. B., Hua, Q., and Liu, H. (2024). "Insights into activators on biomass-derived carbon-based composites for electrochemical energy storage," *Materials Today Chemistry* 37, article 101988. <https://doi.org/10.1016/j.mtchem.2024.101988>

Lv, H., Xiao, Z., Zhai, S., Wang, X., Hao, J., Tong, Y., and An, Q. (2023). "Ni<sub>3</sub>S<sub>2</sub> nanoparticles encapsulated in S-doped biomass-derived hierarchically porous carbon as an advanced electrode for excellent hybrid supercapacitors performance," *Industrial Crops and Products* 194, article 116320. <https://doi.org/10.1016/j.indcrop.2023.116320>

Lv, Y., Huang, L., Chen, C., Cai, Z., and Ruhlmann, L. (2024). "Biomass-derived porous carbon materials for electrocatalysis," *ChemistrySelect* 9(28), article e202401225. <https://doi.org/10.1002/slct.202401225>

Ma, F., Liu, Z., Zhang, G., Xiong, Y., Zhang, M., Zheng, L., Zhen, L., and Xu, C. (2022). "Isolating Fe atoms in N-doped carbon hollow nanorods through a ZIF-phase-transition strategy for efficient oxygen reduction," *Small*, 18(49), article 2205033. <https://doi.org/10.1002/smll.202205033>

Ma, Y., Ke Ping, Sun, P., Lin, K., Guo, J., Yue, L., Zhang, W., Wu, X., and Wen, Z. (2025). "SnO<sub>2</sub>-SnS<sub>2</sub>/graphene heterojunction composite promotes high-performance sodium ion storage," *Journal of Materomics* 11(4), article 100983. <https://doi.org/10.1016/j.jmat.2024.100983>

Macchi, S., Watanabe, F., Viswanathan, T., and Siraj, N. (2021). "Characterization and electrocatalytic performance of molasses derived co-doped (P, N) and tri-doped (Si, P, N) carbon for the ORR," *Electrochem* 2(2), 311-322. <https://doi.org/10.3390/electrochem2020022>

Miao, L., Wang, Z., Gao, M., Peng, J., Chen, Y., Chen, F., Chen, W., and Ao, T. (2024). "A green potassium citrate activation strategy via one-step synthesis of 3D porous carbon for capacitive deionization," *Separation and Purification Technology* 346, article 127510. <https://doi.org/10.1016/j.seppur.2024.127510>

Mukherjee, A., Patra, B. R., Podder, J., and Dalai, A. K. (2022). "Synthesis of biochar from lignocellulosic biomass for diverse industrial applications and energy harvesting: Effects of pyrolysis conditions on the physicochemical properties of biochar," *Frontiers in Materials* 9, article 870184. <https://doi.org/10.3389/fmats.2022.870184>

Ou, J., Zhang, H., Lei, Y., Li, K., Li, B., Deng, H., Wang, H., and Zou, L. (2023). "Buckwheat core derived nitrogen- and oxygen-rich controlled porous carbon for high-performance supercapacitors," *Journal of Central South University* 30(2), 419-433. <https://doi.org/10.1007/s11771-023-5249-0>

Roy, N., Anil Kumar, Y., Ramachandran, T., Fouda, A. M., Hegazy, H. H., Moniruzzaman, M., and Woo Joo, S. (2025). "Biomass-derived nanostructures and hydrothermal carbon spheres: A review of electrochemical applications in redox flow battery," *Journal of Industrial and Engineering Chemistry* 144, 228-254. <https://doi.org/10.1016/j.jiec.2024.10.017>

Sang, J., Sun, C., Pan, J., Gao, C., Zhang, R., Jia, F., Wang, F., and Wang, Q. (2024). "Seaweed-modification of Si by natural nitrogen-doped porous biochar for high-efficiency lithium batteries," *ACS Applied Materials & Interfaces* 16(9), 11389-11399. <https://doi.org/10.1021/acsami.3c15459>

Shang, Z., An, X., Zhang, H., Shen, M., Baker, F., Liu, Y., Liu, L., Yang, J., Cao, H., Xu, Q., Liu, H., and Ni, Y. (2020). "Houttuynia-derived nitrogen-doped hierarchically porous carbon for high-performance supercapacitor," *Carbon* 161, 62-70. <https://doi.org/10.1016/j.carbon.2020.01.020>

Sruthy, E. S., Grimm, A., Paul, M., Cherian, C. T., Thyrel, M., Molaiyan, P., Lassi, U., Petnikota, S., and Reis, G. S. D. (2025). "Low-temperature highly graphitized porous biomass-based carbon as an efficient and stable electrode for lithium-ion batteries and supercapacitors," *Chemical Engineering Journal Advances* 22, article 100762. <https://doi.org/10.1016/j.ceja.2025.100762>

Tariq, M., Ahmed, K., Khan, Z., and Sk, M. P. (2025). "Biomass-derived carbon dots: Sustainable solutions for advanced energy storage applications," *Chemistry – An Asian Journal* 20(9), article e202500094. <https://doi.org/10.1002/asia.202500094>

Wang, J., Nie, P., Ding, B., Dong, S., Hao, X., Dou, H., and Zhang, X. (2017). "Biomass derived carbon for energy storage devices," *Journal of Materials Chemistry A* 5(6), 2411-2428. <https://doi.org/10.1039/C6TA08742F>

Wang, K., Wu, M., Chen, Y., Wen, Y., Li, L., Zhou, W., Sun, F., and Su, X. (2025). "Closed nanopore engineering of hard carbon for enhanced sodium plateau storage: A review and prospects," *Small* 21(52), article e10643. <https://doi.org/10.1002/smll.202510643>

Wang, L., Feng, X., Li, X., Wang, H., Wu, J., Ma, H., and Zhou, J. (2022a). "Hydrothermal, KOH-assisted synthesis of lignin-derived porous carbon for supercapacitors: Value-added of lignin and constructing texture properties/specific capacitance relationships," *Journal of Materials Research and Technology* 16, 570-580. <https://doi.org/10.1016/j.jmrt.2021.12.040>

Wang, M., He, D., Zhu, M., Wu, L., Wang, Z., Huang, Z.-H., and Yang, H. (2023). "Green fabrication of hierarchically porous carbon microtubes from biomass waste via self-activation for high-energy-density supercapacitor," *Journal of Power Sources* 560, article 232703. <https://doi.org/10.1016/j.jpowsour.2023.232703>

Wang, R., Wang, P., Yan, X., Lang, J., Peng, C., and Xue, Q. (2012). "Promising porous carbon derived from celtuce leaves with outstanding supercapacitance and CO<sub>2</sub> capture performance," *ACS Applied Materials & Interfaces* 4(11), 5800-5806. <https://doi.org/10.1021/am302077c>

Wang, S., Wu, Y., Zhang, X., Liu, X., Zhang, W., and Kong, W. (2022b). "Hierarchical porous carbon fabricated by NaCl-activated *Artemisia argyi* rod as electrode material for high-performance supercapacitor," *Ionics* 28(6), 2991-3000. <https://doi.org/10.1007/s11581-022-04551-1>

Wu, J., Song, A., and Li, Y. (2024). "Advances in the applications of biomass-derived carbon materials in triboelectric nanogenerators," *Energy Environmental Protection* 38(6), 47-58. <https://doi.org/10.20078/j.eep.20240304>

Wu, K., Zhang, L., Yuan, Y., Zhong, L., Chen, Z., Chi, X., Lu, H., Chen, Z., Zou, R., Li, T., Jiang, C., Chen, Y., Peng, X., and Lu, J. (2020). "An iron-decorated carbon aerogel for rechargeable flow and flexible Zn-air batteries," *Advanced Materials*, 32(32), article 2002292. <https://doi.org/10.1002/adma.202002292>

Xu, B., Qi, S., Li, F., Peng, X., Cai, J., Liang, J., and Ma, J. (2020a). "Cotton-derived oxygen/sulfur co-doped hard carbon as advanced anode material for potassium-ion batteries," *Chinese Chemical Letters* 31(1), 217-222. <https://doi.org/10.1016/j.cclet.2019.10.009>

Xu, L., Li, X., and Li, X. (2020b). "Large-sized and ultrathin biomass-derived hierarchically porous carbon nanosheets prepared by a facile way for high-performance supercapacitors," *Applied Surface Science* 526, article 146770. <https://doi.org/10.1016/j.apsusc.2020.146770>

Yang, D., Li, S., Cheng, D., Miao, L., Zhong, W., Yang, X., and Li, Z. (2021). "Nitrogen, sulfur, and phosphorus codoped hollow carbon microtubes derived from silver willow blossoms as a high-performance anode for sodium-ion batteries," *Energy & Fuels* 35(3), 2795-2804. <https://doi.org/10.1021/acs.energyfuels.0c04258>

Yang, H., Lin, H., Yang, C., Hu, H., Dong, H., Liu, Y., Liu, X., Cui, J., and Xiao, Y. (2024). "Structural regulation of carbon materials through hydrothermal mixing of

biomass and its application in supercapacitors," *Journal of Energy Storage* 83, article 110688. <https://doi.org/10.1016/j.est.2024.110688>

Yu, J., Li, X., Cui, Z., Chen, D., Pang, X., Zhang, Q., Shao, F., Dong, H., Yu, L., and Dong, L. (2021). "Tailoring in-situ N, O, P, S-doped soybean-derived porous carbon with ultrahigh capacitance in both acidic and alkaline media," *Renewable Energy* 163, 375-385. <https://doi.org/10.1016/j.renene.2020.08.066>

Zhan, Z., Zhang, J., Lin, L., Jiang, T., and Shi, J. (2025). "Salt-templated two-step activation synthesis of poplar-derived hierarchical porous carbon for high-performance supercapacitor electrodes," *Industrial Crops and Products* 236, article 122105. <https://doi.org/10.1016/j.indcrop.2025.122105>

Zhang, S., Li, X., Gao, Y., Li, L., Bao, L., and Li, X. (2025). "Physicochemical double protection enables stable MXene for high-rate performance hybrid supercapacitors," *Journal of Materials Science & Technology* 211, 89-97. <https://doi.org/10.1016/j.jmst.2024.05.053>

Zhao, W., Deng, J., Li, M., Du, G., Fan, M., Gao, H., and Yuan, Z. (2025a). "Rational synthesis of sea urchin-like NiCo-LDH/tannin carbon microsphere composites using microwave hydrothermal technique for high-performance asymmetric supercapacitor," *Advanced Composites and Hybrid Materials* 8(2), article 215. <https://doi.org/10.1007/s42114-025-01220-5>

Zhao, X., Wang, X., Gao, P., Zhao, P., Wang, J., Li, Y., Han, Z., and Shen, B. (2025b). "Eco-friendly synthesis coupled with predictive analytics: Developing hierarchical lignin-derived ordered mesoporous carbon for advanced supercapacitors," *Green Energy & Environment* 10(6), 1256-1269. <https://doi.org/10.1016/j.gee.2024.11.006>

Zhong, Z., Shao, Q., Ni, B., Wang, D., Xie, Z., Xu, L., Mu, Y., Wang, Q., Wang, T., Feng, Y., Hou, J., Jiang, K., Cheetham, A. K., and Wang, T. (2025). "HOF-enabled synthesis of porous PEDOT as an improved electrode material for supercapacitor," *ACS Applied Materials & Interfaces* 17(10), 15804-15812. <https://doi.org/10.1021/acsami.4c19109>

Zhu, M., Yang, Y., and Ma, Y. (2023). "Salt-assisted synthesis of advanced carbon-based materials for energy-related applications," *Green Chemistry* 25(24), 10263-10303. <https://doi.org/10.1039/D3GC03080F>

Zhu, Z., Li, Y., Li, X., Qiu, H., Fang, L., Zheng, L., Gao, J., and Zhu, G. (2024). "Efficient ORR catalyst: porous activated carbon prepared from water hyacinth with high N content," *Journal of Nanoparticle Research* 26(5), article 93. <https://doi.org/10.1007/s11051-024-06005-3>

Article submitted: August 14, 2025; Peer review completed: December 13, 2025; Revised version received: January 30, 2026; Accepted: January 31, 2026; Published: February 5, 2026.

DOI: 10.15376/biores.21.2.Wang